Journal for ImmunoTherapy of Cancer

Oncolytic vesicular stomatitis virus–based cellular vaccine improves triple-negative breast cancer outcome by enhancing natural killer and CD8+ T-cell functionality

Seyedeh-Raheleh Niavarani,[1] Christine Lawson,[1] Marie Boudaud,[2] Camille Simard,[3] Lee-Hwa Tai [1,4]

To cite: Niavarani S-R, Lawson C, Boudaud M, *et al*. Oncolytic vesicular stomatitis virus–based cellular vaccine improves triple-negative breast cancer outcome by enhancing natural killer and CD8+ T-cell functionality. *Journal for ImmunoTherapy of Cancer* 2020;**8**:e000465. doi:10.1136/jitc-2019-000465

► Additional material is published online only. To view please visit the journal online (http://dx.doi.org/10.1136/jitc-2019-000465).

Accepted 14 February 2020

For numbered affiliations see end of article.

Correspondence to
Dr Lee-Hwa Tai;
lee-hwa.tai@usherbrooke.ca

BACKGROUND

The occurrence of triple-negative breast cancer (TNBC) is significant, with an estimated 40,000 cases diagnosed in US women each year (American Cancer Society, 2018). TNBC is a vastly heterogeneous disease that are grouped together histologically since they lack hormone and Her-2 receptors. However, TNBC is best considered as an umbrella term, encompassing a wide spectrum of entities with distinct genetic, transcriptional, histological and clinical differences.[1–3] As a group, TNBC is associated with high proliferation, early recurrence and poor survival rates.[2 4] This aggressive disease is resistant to widely used targeted therapies such as trastuzumab and endocrine therapies, which have been effective at reducing breast cancer mortality. The best chance for survival is early detection, followed by neoadjuvant chemotherapy (NAC) and surgical resection.[5] Patients with early-stage TNBC have increased rates of pathologic complete response (pCR) after NAC compared with other breast cancer subtypes. Indeed, the best prognostic factor for TNBC is the patient's response to NAC. However, the increased pCR rates, but worse survival observed in TNBC—termed the *triple negative paradox*—appears to be driven by higher relapse rates among those patients whose tumors are not eradicated by chemotherapy.[2 5] There are very limited and often ineffective treatment options for patients with poor prognosis (chemoresistant and late-stage/metastatic) TNBC.[2]

Recent large-scale gene expression profiling and immunohistochemistry (IHC) analyses reveal that TNBC may be the most regulated by tumor-infiltrating lymphocytes (TILs) and thus the most responsive to immunotherapies compared with other breast cancer subtypes.[6 7] In addition, accumulating data suggest that certain chemotherapeutic drugs such as anthracyclines mediate their anti-cancer activity through direct cytotoxic effects and also through activation of TIL responses.[8] The presence of TILs suggests an immune response to tumor-associated antigens (TAAs). Several studies have evaluated TILs in breast cancer specimens and a higher level of TILs has been reported in TNBCs compared with other breast cancer subtypes.[9] Furthermore, TNBC is characterized by genomic instability and high rates of genetic mutations, which implicate the production of more neoantigens and increased immunogenicity.[10 11] Pivotal gene expression profiling studies carried out by Lehmann *et al*[12–14] revealed the existence of six subtypes of TNBC, namely basal-like 1, basal-like 2, immunomodulatory, mesenchymal, mesenchymal stem-like and luminal androgen receptor. While these first-generation signatures revealed the transcriptional heterogeneity of TNBC, second-generation prognostic signatures based on immune response–related genes allowed for the stratification of patients with TNBC according to overall and relapse-free survival. Recently, a gene expression analysis of immune activating and suppressive factors in TNBC of the GeparSixto study showed three subgroups of tumors, immune group A, B and C with low, intermediate and high immune gene expression levels, respectively. Importantly, immune group C tumors had a higher extent of TIL infiltrate and better pCR rates compared with tumors from immune groups A and B. Furthermore,

the extent of TILs in residual TNBC following NAC has been associated with improved overall and relapse-free survival, highlighting the potential of TIL as a biomarker in the post-adjuvant setting to identify patients at risk of relapse.[8 15 16] Taken together, these studies provide strong rationale to therapeutically target poor prognosis TNBC with novel immunotherapies, such as immunogenic tumor cell vaccines.

Infusion of inactivated whole tumor cells, extracted from a patient's own tumor (autologous), represents a truly personalized treatment option for malignancies with no targeted therapies, such as TNBC. Currently, many immunotherapeutic strategies designed to activate TNBC TILs are being tested in preclinical and clinical studies. Among them are the use of vaccines against cancer testis antigens (MAGE-A, NY-ESO-1) and other TAAs. Recent IHC and gene expression data show more frequent expression of these TAAs in TNBC versus other subtypes.[6 16] Given that TNBC is a highly heterogeneous disease, it logically follows that not all patients will benefit from a vaccine strategy targeting a single TAA. On the other hand, treatment with autologous tumor cells will expose a patient with TNBC to their complete and individualized TAA repertoire. Importantly, the multiple personalized epitopes contained within the autologous vaccine can potentiate a polyclonal immune response capable of eliminating a diverse population of heterogeneous TNBC tumors.[17] However, whole tumor cell vaccines have demonstrated limited success in clinical trials, mainly due to lack of immunogenicity.[17 18] Furthermore, many tumors downregulate their expression of MHC or costimulatory molecules, which are both needed to generate a robust adaptive immune response.

We and others have endeavored to improve on the whole tumor cell vaccination paradigm by infecting harvested tumor cells ex vivo with engineered oncolytic viruses (OVs) followed by direct delivery into the tumor microenvironment.[19–22] This approach avoids the major barriers to systemic OV delivery and allows further ex vivo modification of the tumor cells to improve immunogenicity.[16 17] Recombinant Vesicular Stomatitis Virus (VSVd51) is a genetically modified rhabdovirus with a point mutation in the matrix protein, which expands its tropism for diverse cancer types, breast cancer included, and greatly attenuates its replication in healthy tissue when compared with other OVs.[23] Specifically, the VSV M protein mutation improves its therapeutic index by preventing viral blockade of host cell transcription and nucleocytoplasmic transport, including interferon (IFN) production.[24–26] Following infection with VSVd51, healthy cells with intact IFN signaling pathways are protected, while malignant cells, which have lost the ability to mount an IFN response, remain susceptible.[24 27 28] Importantly, the lack of pre-existing neutralizing antibodies in human populations, a major hurdle that impedes the in vivo delivery of many other OVs (herpes, vaccinia, measles), warrants the development of oncolytic rhabdoviruses for clinical applications.[29 30] Schirrmacher's group provided the first proof of concept for an ex vivo infected tumor cell vaccine approach using oncolytic Newcastle Disease Virus to effectively treat colorectal tumors,[31 32] while Conrad *et al*[33] and Lemay *et al*[22] demonstrated efficacy in L1210 leukemic and B16 melanoma models, respectively.

We recently demonstrated that the intratumoral delivery of autologous colon cancer cells infected with an attenuated rhabdovirus (MG1) provided a significant therapeutic benefit to normally resistant mouse models of established peritoneal disease.[19] A whole cell vaccine infected with MG1 was well tolerated by mice while inducing a robust recruitment of cytotoxic natural killer (NK) and T cells to the peritoneal cavity that was associated with robust long-term survival.[19] However, in the setting of developing human TNBC that have already escaped the protective immune response, it is unlikely that ICV alone will be effective. A combination of surgery, chemotherapy along with novel small molecule inhibitors and monoclonal antibodies are currently administered to patients with TNBC in clinical trials with the goal of eradicating cancer and eliminating recurrence due to resistant or mutated TNBC cells.[2 34] In the phase III Impassion 130 trial, a positive median overall survival (OS) was observed in patients with TNBC receiving anti-PD-L1 atezolizumab with nab-paclitaxel, compared with patients receiving nab-paclitaxel plus placebo.[1 35] Given the importance of activating TILs in the immunosuppressive TNBC microenvironment and the high therapeutic potential of immunogenic cancer vaccines, we propose to develop and characterize an oncolytic VSVd51-based cancer vaccine in combination with anti-PD-1 checkpoint inhibitor to treat poor prognosis TNBC in the postoperative setting.

METHODS

Cell lines and viruses

4T1 and MDA-MB-231 were maintained in DMEM; BT-549 in RPMI, all supplemented with 10% heat inactivated FBS+100 U/mL penicillin and 100 µg/mL streptomycin (P/S). All cell lines were purchased from ATCC in the past year and were verified to be mycoplasma free and show appropriate microscopic morphology at time of use. VSVd51 expressing GFP was propagated on Vero cells and purified using Opti-Prep purification methods. Viral titers were determined by a standard plaque assay as previously published.[19] Viral cytotoxicity was assessed on the indicated cell lines, and cell viability was carried out as described previously.[19]

Mice

Female BALB/c mice (6–8 weeks old, 20–25 g) were purchased from Charles Rivers (Quebec). Animals were housed in pathogen-free conditions at the Central Animal Facility of the Université de Sherbrooke with access to food/water ad libitum. Animals were euthanized by cervical dislocation under anesthesia. All studies

were conducted in accordance with university guidelines and the Canadian Council on Animal Care.

4T1 syngeneic mouse model with resection and vaccination

We have previously developed and validated a mouse model of spontaneous metastasis and surgical resection of primary TNBC.[36 37] At day 0, 1×10^5 4T1 cells in 100 µL (>98% viability) were injected orthotopically into the fourth mammary fat pad of BALB/c mice. Following tumor implantation, mice were monitored daily by palpation of the injection site, the volume of palpable tumors were measured by a Vernier caliper and the tumor volume was calculated via the equation (width^2×length)/2. At days 12–14, a complete resection of the primary tumor was performed (tumor volume=75–80 mm^3). During surgery, all mice were kept under anesthesia (3% induction, 1.5% maintenance of isoflurane with 2% O_2). For perioperative pain management, all mice were injected with 0.05 mg/kg of buprenorphine 1 hour before and 4 hours following surgery. Mice were randomized into different cohorts for treatment. At 1 day and 3 days following surgery, irradiated 4T1 cells, infected cell vaccine (4T1-ICV), VSVd51 alone or sterile PBS was injected subcutaneously into the cleared mammary fat pad. For the in vivo depletion of immune cell populations, 6 doses of depletion antibodies (1 dose 24 hours before surgery, followed by 5 additional doses 2–3 days apart) were administered by intraperitoneal injection at 20 µg/dose for anti-Asialo (GM1; Life Technologies) and 250 µg/dose for anti-CD8α (53-6.7; BioXCell). For anti-PD-1 treatment, mice were injected intraperitoneally with 1 dose of anti-PD-1 (RMP1-14; BioXCell) at 100 µg/dose, followed by 1 additional dose 3 days later.

TNBC patient tumor dissociation

TNBC tissue from patients were collected after surgery and placed in DMEM supplemented with 10% heat inactivated FBS+P/S. Tumors were dissociated using the human tumor dissociation kit (Miltenyi biotec) according to the manufacturer's recommendations. Briefly, tumors were cut into small pieces (<2 mm^3), then treated with enzymes and placed into the gentle MACS OctoDissociator (Miltenyi biotec). Macroscopic pieces were removed using 70 µm cell strainers. Tumor cells were washed twice in DMEM. Cells were viably frozen down or freshly used for downstream experiments.

ICV preparation

ICV using VSVd51 was prepared as previously published.[19] Viable single cell suspensions (5×10^6) of 4T1 primary tumors were γ-irradiated at 50 Gy. This range of cell number and irradiation has been previously determined to create a non-proliferating but intact whole-cell vaccine.[22] VSVd51 was added to the cells at 5×10^7 plaque-forming units (PFU) and further incubated at 37°C for 24 hours. This preparation was injected subcutaneously in mice at 100 µL, giving each mouse 1:10 γ-irradiated cells to virus per dose (10 multiplicity of infection, MOI).

Flow cytometry

Antibodies are listed in online supplementary table S1. To analyze mouse spleen and blood lymphocyte populations, an initial incubation was done in ACK lysis buffer for 5 min to lyse red blood cells. A total of 1×10^6 splenocytes or blood cells were then added to each tube. Fc block was added prior to antibody staining for 20 min at 4°C. Samples were washed twice with flow cytometry buffer (PBS+2% FBS) and acquired on a CytoFLEX 30 (Beckman Coulter). Data were analyzed with CytExpert software. For assessment of NK and T-cell functionality, fresh blood or spleen lymphocytes were cultured with VSVd51-infected 4T1 cell lysates for 4 hours in the presence of brefeldin A (1 µL/mL) at 37°C. After 4 hours, cells were washed twice with PBS, and then stained for NK and T-cell markers (online supplementary table S1). Cells were then fixed and permeabilized using BD Cytofix/Cytoperm kit, according to the manufacturer's protocol, and intracellular staining for granzyme B and IFNγ was performed. For CD107a, the antibody was added to cells in the beginning for cell-surface staining of CD107a on degranulation, as described previously.

Immunogenic cell death (ICD) assays

Conditioned media (CM) was obtained by seeding 5×10^5 cells in 24-well plates in their corresponding media for 24 hours followed by infection with VSVd51 at the indicated PFU for the indicated time points. *Flow cytometry*: infected cells were harvested and processed as described above. Antibodies are listed in online supplementary table S1. Bioimaging was performed using a fluorescence microscope (Leica). *Western blot*: proteins from CM (HMGB1) or cell lysates (for other proteins) were resolved by SDS-PAGE and transferred to Immun-Blot-PVDF membranes (BioRad) for immunoblotting. Protein expression was detected using specific primary antibodies (1:1000) and corresponding HRP-conjugated secondary antibodies (1:10,000). Protein expression was visualized by chemiluminescence detection (ChemiDoc; BioRad). All antibodies are listed in online supplementary table S1. For *ATP detection*, the relative concentration of ATP in the CM was measured with the ENLITEN-ATP kit (Promega). Briefly, 100 µL of CM was transferred to 96-well opaque plates. Then 100 µL of reconstituted rLuciferase/Luciferin reagent was added to each well followed by measurement of luciferase using a luminescence microplate reader (Fusion V.3.0).

Transmission electron microscopy (EM)

Seventy-two hours following infection with VSVd51, TNBC cells were harvested and provided to the histological platform (Université de Sherbrooke) for processing and imaging. Briefly, cells were fixed in 2.5% cacodylate-buffered glutaraldehyde for a minimum of 2 hours. Cells were then centrifuged and the pellet resuspended in sodium cacodylate buffer (pH 7.2), post-fixed in 2% osmium tetroxide for 2 hours and dehydrated up to absolute ethanol concentrations. A final dehydration in pure

acetone was followed by three changes in Spurr's resin and a final embedding at 65°C. Then 80 nm sections were cut using a Leica Ultracut UCT and stained with uranyl acetate and lead citrate. Grids were screened on a Hitachi 7500 Transmission EM and the images were digitally captured.

Quantitative PCR (qPCR)

Total RNA from infected mouse and human TNBC cell lines and single cell suspensions of patient TNBC tissue were extracted using Trizol (Invitrogen) and cDNA was prepared using the QuantiTect Reverse Transcription Kit (Qiagen) from 1.2 µg of total RNA in the presence of 20 IU of RNAseOUT (Invitrogen). Target transcripts were quantified by qPCR by cDNA amplification with Taq Polymerase (Feldan Bio) and SYBR Green I (Millipore Sigma) according to the manufacturer's instructions. All primers were purchased from Integrated DNA Technologies and are listed in online supplementary table S2. Target gene expression was normalized to housekeeping genes 18S ribosomal proteins for human cell lines and tissue samples or to Rplp0 ribosomal protein for mouse cell lines. Transcript levels were calculated using the ΔΔCT (cycle threshold) method and results were displayed as fold change of infected samples relative to uninfected samples. Genes were additionally visualized on 2% agarose gel to confirm their expression if basal levels were not detected.

Enzyme-linked immunosorbent assays

Culture supernatants were diluted fivefold. ELISA kits for detecting mouse CXCL10, CCL5, CCL2 and CCL4 were purchased from Peprotech and performed according to the manufacturer's instructions.

Human polarization, proliferation and migration assays

Polarization: human monocytes were isolated from peripheral blood (Human $CD14^+$ isolation kit; Stemcell). Then 5×10^5 monocytes were seeded in 24-well plates in complete RPMI and incubated overnight at 37°C and 5% CO_2. Twenty-four hours later, the monocyte media was replaced with the CM of infected human cell lines. For controls, monocytes were co-cultured with recombinant human IL-10, IL-4 and TGFβ (BioBasic) all at a final concentration of 20 ng/mL for differentiation to M2-like macrophages; and with lipopolysaccharides (50 ng/mL) (Millipore Sigma) and recombinant human IFNγ (20 ng/mL) (BioBasic) for M1-like macrophages. Undifferentiated monocytes remained in complete media as M0. Following overnight incubation, cells were harvested and processed for flow cytometry as described above. Antibodies are listed in online supplementary table S1. *Proliferation*: monocytes from the polarization assay were further incubated with carboxyfluorescein succinimidyl ester (CFSE)–labeled (3 µM; BD Horizon) human peripheral blood mononuclear cells (PBMCs) for 5 days in the presence of plate-bound anti-CD3 (OKT3, 5 µg/mL) and anti-CD28 (CD28.2, 2 µg/mL). Cells were harvested and stained with anti-CD3 (HIT3a), anti-CD8 (SK1) for flow cytometric analysis of CFSE dilution. *Migration:* 200 µL of CM was placed in the lower well of Boyden chambers, separated from the top well by a 5 mm pore polycarbonic membrane (Neuro Probe). Then 6×10^5 human PBMCs was added to the top chamber, followed by incubation at 37°C, 5% CO_2 for 45 min. Next, the media in the top of the chamber was aspirated and the membrane removed with forceps. This was followed by harvesting of media in the bottom chamber and quantification of migrated cells by Trypan Blue exclusion. The cells were stained and acquired by flow cytometry as described above.

Histological analysis

Lungs from treated mice were harvested and fixed in 4% formaldehyde for 24 hours and kept in ethanol for analysis. Lungs were then embedded in paraffin and 5 µm sections were used for immunofluorescence staining using CD3, IFNγ and granzyme B. All antibodies are listed in online supplementary table S1. Slides were scanned using a digital slide scanner (Nanozoomer-XR C12000; Hamamatsu) provided by the Histology Platform (Université de Sherbrooke). Percentage staining of marker-positive areas were quantified using ImageJ software (NIH).

Statistical analysis

All statistical analyses were generated using Prism V.7 (GraphPad). Unpaired two-tailed t-tests were used for comparing uninfected or infected cells or differentially treated mice. Survival differences of tumor-bearing and treated mice were assessed using Kaplan-Meier curves and analyzed by log-rank testing. P value <0.05 was considered as statistically significant.

RESULTS

Necrotic phenotype accompanies TNBC cell death following infection with VSVd51

We previously demonstrated that an autologous rhabdovirus ICV elicited profound anti-tumor immune responses in B16 melanoma and CT26 peritoneal carcinomatosis preclinical models.[19] Given the lack of therapeutic options for poor-prognosis TNBC, we proposed to develop an adjuvant ICV to prevent relapse and reduce metastases in this aggressive disease. We used rhabdoviral VSVd51 expressing enhanced green fluorescence protein (GFP) and first assessed its cytotoxic activity in mouse and human TNBC cells. VSVd51 was able to infect mouse 4T1 and human MDA-MB-231 and BT-549 cells as shown by GFP expression following 72 hours of infection with 10 MOI (figure 1A) and induce cellular cytotoxicity over a range of increasing MOI as measured by a MTT assay (figure 1C). Given the importance of the mode of tumor cell death in initiating anti-tumor immune responses,[38 39] we investigated cell death features following infection of TNBC cells with VSVd51. We first examined cellular morphology using transmission EM (figure 1B). Condensed nuclear structures, cytoplasmic vacuoles and

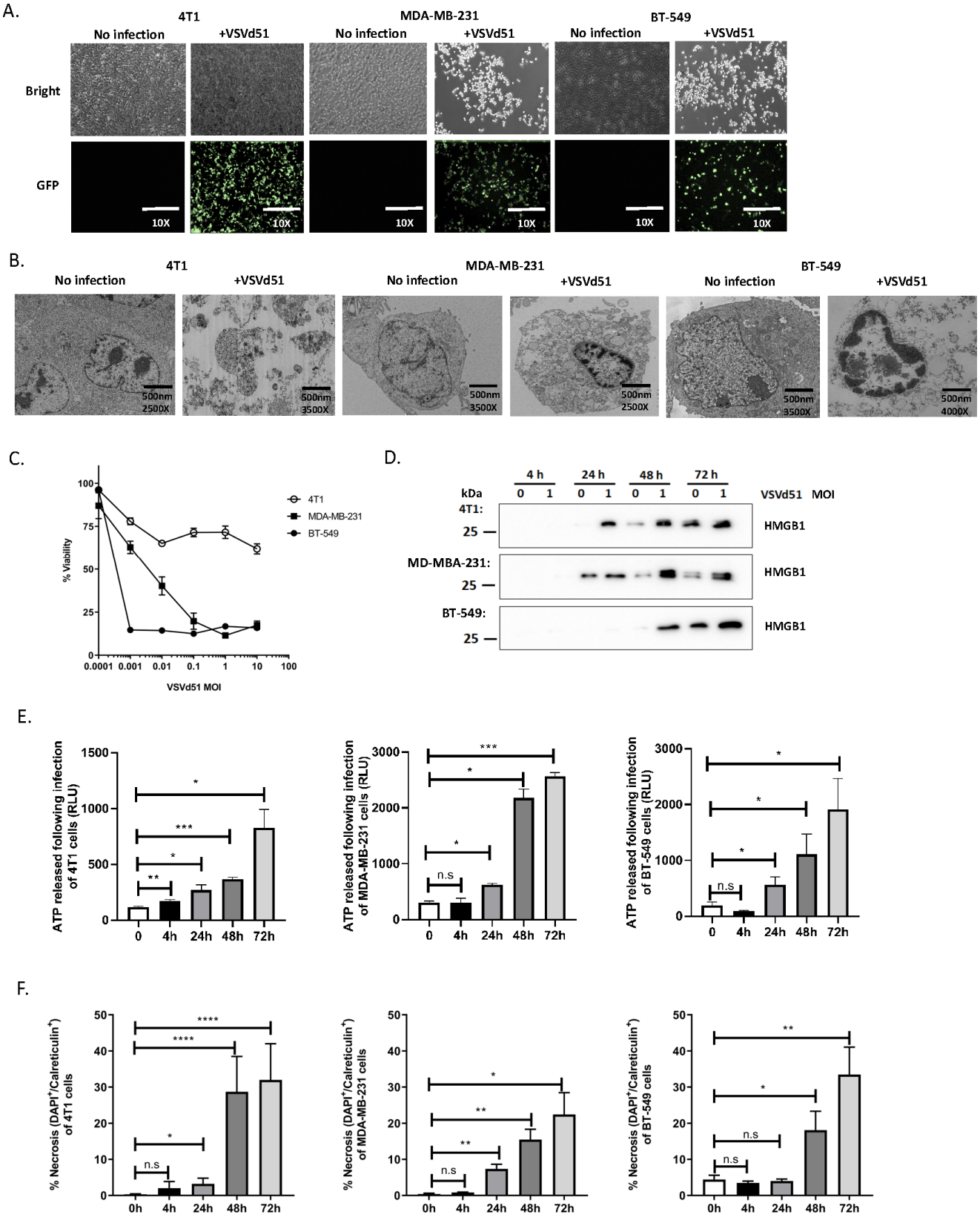

Figure 1 Necrotic phenotype accompanies triple-negative breast cancer (TNBC) cell death following infection with VSVd51. (A) Light microscopy images of TNBC cell lines infected with 10 multiplicity of infection (MOI) of VSVd51 for 24 hours. (B) Electron microscopy images of TNBC cell lines infected with 10 MOI of VSVd51 for 72 hours. (C) Cell viability assay, (D) Western blot analysis of HMGB1 from cell-free supernatants, (E) luminometry measurement of relative ATP from cell-free supernatants and (F) measurement of cell surface calreticulin of TNBC cell lines infected with VSVd51 at indicated MOI and following indicated time points. All data are representative of at least three similar experiments where n=3 for technical replicates, *p<0.05; **p<0.01; ***p<0.001; ****p<0.0001; n.s., not significant.

ruptured cellular membranes were observed. Next, we detected high mobility group box 1 (HMGB1) protein (figure 1D) and ATP (figure 1E) in the supernatant of VSVd51-infected cells at various time points post-infection, suggesting passive release from necrotic cells. Another feature of necrosis is the presence of cell surface externalized calreticulin. Following VSVd51 infection, we observed an increase in the percentage of necrotic (calreticulin$^+$/DAPI$^+$) cells in all tested cell lines at 48 and 72 hours post-infection (figure 1F). Together, the presence of these danger-associated molecular patterns (DAMPs) suggest a necrosis-like phenotype of TNBC cells following VSVd51 infection. Features of classical apoptosis (Annexin V$^+$/DAPI$^-$, Caspase-3 and PARP cleavage) were minimally or not observed (online supplementary figure 1A,B). In addition, the autophagic flux was blocked by bafilomycin treatment and no differences in the conversion of LC3-I to LC3-II was observed following VSVd51 infection in all cell lines tested. This suggests that VSVd51 infection of TNBC cells does not lead to autophagic cell death (online supplementary figure 1C). By comparison, treatment of TNBC cells with doxorubicin, a clinically relevant neoadjuvant chemotherapeutic for TNBC, revealed that VSVd51 induced greater release of HMGB1 and calreticulin exposure (online supplementary figure 1D,E).

Immunogenic gene signature is detected on TNBC cells after infection with VSVd51

Next, we sought to determine if VSVd51-induced necrosis is immunogenic in nature. To accomplish this, we examined a panel of genes related to pro-inflammatory, anti-inflammatory, antigen presentation and immune differentiation markers by qPCR. Following overnight infection with VSVd51, we detected a general upregulation of genes related to immune cell recruitment and activation in mouse and human TNBC cell lines tested. Notably, mouse CCL2, CCL4, CCL5, CXCL10, IL-6 and MHC-I related genes showed an increase in expression in 4T1 cells following infection compared with non-infected controls (figure 2A). The expression of several top immunogenic genes (CCL2, CCL4, CCL5 and CXCL10) at the protein level were measured by ELISA in 4T1 cells following infection to support the gene expression data (online supplementary figure 2A). In human MDA-MB-231 and BT-549 cell lines, CCL5, CXCL2, IRF-1 and MHC-I genes were upregulated (figure 2B,C). Genes were additionally visualized on 2% agarose gel to confirm their expression if basal levels were not detected. Notably, IFNγ, IL-2 and PD1 genes were induced following infection in 4T1 cells (online supplementary figure 2B), while CSF-1, CCL4 and CXCL10 were induced in BT-549 and MDA-MB-231 infected cells (online supplementary figure 2C,D). These data suggest that an immunogenic gene signature is present in TNBC cells following VSVd51-induced necrotic cell death.

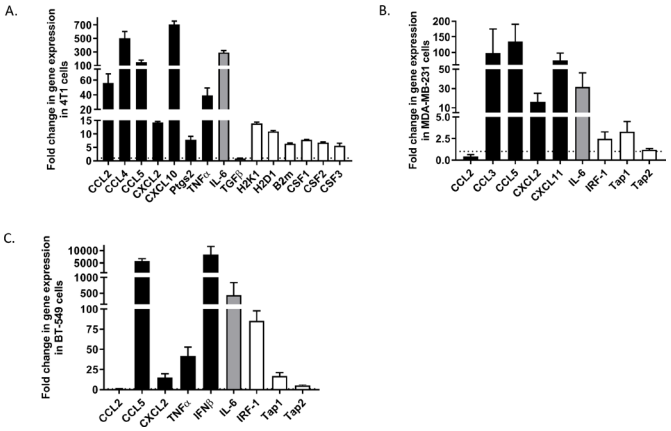

Figure 2 Immunogenic gene signature is detected on triple-negative breast cancer (TNBC) cells after infection with VSVd51. Fold change in gene expression of (A) mouse 4T1, human (B) MDA-MB-231 and (C) BT-549 TNBC cells following infection with VSVd51 at 10 multiplicity of infection for 24 hours. Quantitative PCR was performed using mRNA pooled from three independent experiments.

Enhanced innate and adaptive immune cell activation by ICV

To determine if the observed in vitro ICD features (figure 1) and gene signatures (figure 2) translate to enhanced immune function in vivo, we tested the ICV in the adjuvant setting in BALB/c mice bearing orthotopic 4T1 tumors following primary tumor resection (figure 3A, timeline). This model makes use of an aggressive mouse stage IV TNBC from the BALB/c strain that spontaneously metastasizes from the mammary glands to multiple distant sites, in particular the lungs. We included the following treatment cohorts (PBS, irradiated 4T1 cells, VSVd51 alone and ICV) to delineate the role of the vaccine's constituent parts. At early and late time points following vaccination, we observed that postoperative vaccination of mice with 2 doses of ICV significantly enhanced the proportion of blood IFNγ$^+$, granzyme B$^+$ (cytotoxicity) and CD107a$^+$ (degranulation) NK cells compared with administration of virus alone, non-infected cells or PBS (figure 3B). Similar results were observed in CD11c$^+$ conventional dendritic cells (DCs) in terms of their overall proportion and activation status (CD86$^+$) (figure 3C). Analysis of both blood and lung CD3$^+$/CD8$^+$ T cells showed enhanced IFNγ, granzyme B and CD107a degranulation in ICV-treated mice over controls (figure 3D,E). Immunofluorescence staining of mice lungs bearing metastatic 4T1 tumors treated with ICV showed increased presence of CD3$^+$ T cells, granzyme B and IFNγ expression compared with lungs from mice treated with irradiated 4T1 cells (figure 3F,G). By comparison with ICV, the addition of a treatment cohort receiving systemic doxorubicin injection, a known ICD inducer, resulted in decreased CD8$^+$ T-cell CD107a degranulation and IFNγ production compared with ICV treatment. Importantly, survival of ICV-treated mice significantly surpassed those cohorts treated with irradiated 4T1 cells or doxorubicin (online supplementary

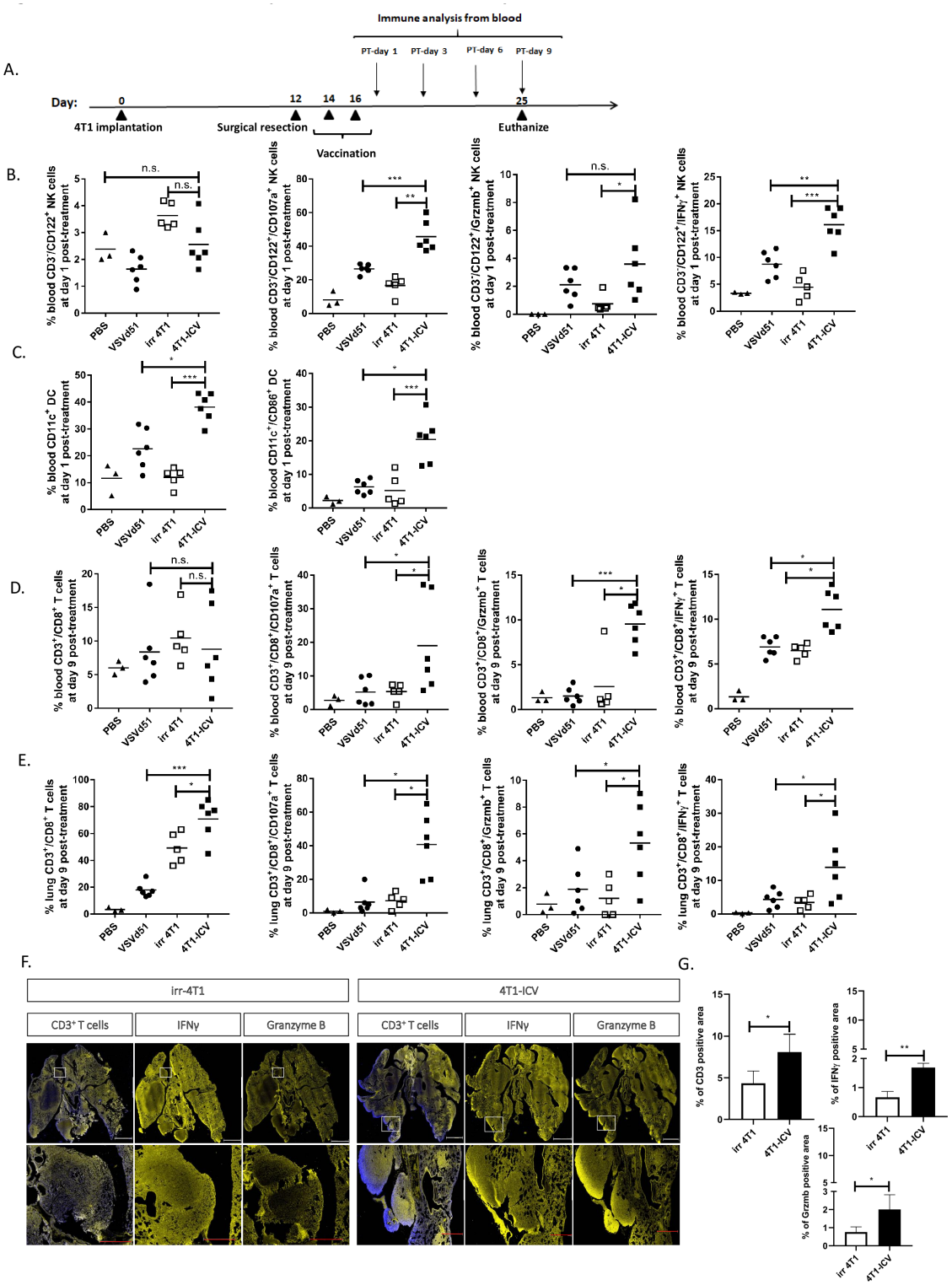

Figure 3 Enhanced innate and adaptive immune cell activation by infected cell vaccine (ICV). (A) Timeline of in vivo BALB/c-4T1 experiment. BALB/c mice were orthotopically implanted with 1×10^5 4T1 cells followed by a complete primary tumor resection on day 12. On days 14 and 16, mice received two doses subcutaneously of either virus alone (VSVd51, MOI=1×10^6 PFU/mL), irradiated cells alone (irr4T1, 5×10^6), an ICV (5×10^6 infected cells) or left untreated (1× PBS). (B–E) Immune cell suspensions from the peripheral blood (B–D) or lungs (E) of mice following indicated treatments were stained with (B) NK cell markers ($CD122^+$, $CD3^-$, $IFN\gamma^+$, granzyme B^+, $CD107a^+$), (C) DC markers ($CD11c^+$, $CD86^+$), (D, E) T-cell markers ($CD3^+$, $CD8^+$, $IFN\gamma^+$, granzyme B^+, $CD107a^+$) and analyzed by flow cytometry. (F) Representative immunofluorescent images and (G) quantification of % expression of $CD3^+$, $IFN\gamma^+$ and granzyme B^+ positive lung area in mice treated with irradiated cells or ICV. Scale: top panel, 2 mm; bottom panel, 0.5 mm. All data are representative of at least three similar experiments where n=3–6 mice/treatment. *p<0.05; **p<0.01; ***p<0.001; n.s., not significant. DC, dendritic cell; MOI, multiplicity of infection; PFU, plaque-forming unit.

figure 3A–C). Taken together, these in vivo data demonstrate the innate and adaptive immune activating capacity of the ICV approach.

CD8+ cytotoxic T cells are critical for ICV efficacy and combination treatment with anti-PD1 checkpoint inhibitor improves survival in the BALB/c-4T1 model

To further investigate the critical role of NK and CD8+ T cells after ICV administration, we monitored for survival in ICV-treated mice that were pharmacologically depleted singly or of both immune cell populations (figure 4A,B). In support of the in vivo data showing enhanced NK and CD8+ T-cell function (figure 3), the protective effect of vaccinated mice with ICV was partially abrogated on depletion of NK cells, but completely abrogated on depletion of CD8+ T cells or combination of NK and CD8+ T cells (figure 4B). These results suggest that the therapeutic benefit of this treatment strategy is dependent on both NK and CD8+ T-cell recruitment, but likely more dependent on CD8+ T cells. Given the importance of CD8+ T cells and their role in mediating the response to ICV treatment, we examined cell surface expression of exhaustion markers on CD8+ T cells at day 9 following ICV treatment and observed augmented levels of PD-1, but not TIM-3 or LAG-3 (figure 4C). In addition, we observed upregulation of PD-L1 expression levels on 4T1 cells following infection with VSVd51 in vitro (figure 4D). These data suggest that the adaptive T-cell response could be modulated to override exhaustion. Therefore, to improve the immune response and survival of vaccinated mice, we combined ICV with anti-PD1 checkpoint inhibitor treatment (figure 4E,F). We observed that combination therapy prolonged survival compared with either monotherapy ICV or anti-PD-1 alone. These preclinical results demonstrate the therapeutic potential of ICV in combination with checkpoint inhibitors to treat TNBC.

Polarization of human monocytes to M1 phenotype and enhanced migration and proliferation of human CD8+ T cells following exposure to ICV

To improve the translational potential of our work, we examined the effect of ICV on human primary antigen-presenting cells. In ex vivo co-culture experiments with CD14+ human monocytes incubated with cell-free lysates derived from infected human TNBC cells, we observed polarization of monocytes toward an M1-like phenotype that have been previously suggested[40 41] to promote anti-tumor immune responses (figure 5A). We additionally examined the activation status of human DC treated ex vivo with the same cell-free lysates (online supplementary figure 4A). ICV-lysate treated DC displayed a more mature phenotype compared with controls. To examine the consequences of ICV-induced M1-like monocytes on effector immune cells, we measured human NK and CD8+ T-cell migration and CD8+ T-cell proliferation in the ex vivo setting. We observed increased migration of NK cells and increased migration and proliferation (CFSE dilution) of CD3+/CD8+ T cells in co-cultures with ICV-lysate treated M1 monocytes (figure 5B,C). Taken together, these data using human primary immune cells and human TNBC cell lines demonstrate the immune activating potential of ICV.

ICV enhances immune signature and biomarkers of ICD in human TNBC patient tissue

To investigate whether the ICV could elicit an immunogenic signature in human TNBC patient tissue, patients with TNBC were enrolled in the VACS study as part of the Sherbrooke Gynecologic Biobank (Ethics no. 2018-2414). Dissociated breast tumor tissue was obtained from two patients with TNBC (BRC1762, BRC1756). The cells were infected with VSVd51 overnight and qPCR for gene expression analysis and assays to measure biomarkers of ICD were conducted. Patient BRC1762 displayed an immunogenic gene expression pattern with enhanced expression of multiple immune genes, notably CCL5, CCL2, CXCL9, CXCL11, CCL3,TGFb, CSF-2, TAP1 and TAP2 (figure 6A). In addition, the genes CCL20, IFNα, IFNβ and GRA that were not basally expressed in uninfected samples showed induced expression following infection with VSVd51. In patient BRC1756, CCL2, CCL5, CXCL2, CCL20, IRF1, TAP1 and TAP2 gene expression were also increased (figure 6B) and the genes CCL20, CTLA-4, CCL3 and CCL4 were induced following infection (online supplementary figure 4B). Biomarkers of ICD including calreticulin cell surface expression (for patient BRC1762) (figure 6C), ATP (figure 6D) and HMGB1 (figure 6E) release for both patients were detected at higher levels in VSVd51-infected cells compared with uninfected controls. These human data demonstrate that an ICD gene signature is present in patient TNBC cells following VSVd51 infection, and this phenotype has the potential of recruiting and activating important immune cells in vivo. Taken together, our translational data highlight the clinical potential of using ICV as adjuvant vaccine to treat patients with TNBC.

DISCUSSION

Given the lack of effective treatments in TNBC, several efforts over the last few years have been made to improve therapeutic opportunities for patients with TNBC, especially for those patients who do not achieve pCR after NAC. In the phase III Impassion 130 trial, a significantly improved progression-free survival (PFS) and a positive median OS was observed in patients with TNBC receiving anti-PD-L1 atezolizumab with nab-paclitaxel, compared with patients receiving nab-paclitaxel plus placebo.[1 35] Preliminary data from the phase Ib/II KEYNOTE-150 trial investigating the combination of anti-PD-1 pembrolizumab with eribulin (microtubule inhibitor) demonstrated substantial benefits in both PFS and OS in the combination treatment arm.[1 42] In addition to combination immune checkpoint and chemotherapy trials, PARP inhibitors are also undergoing early phase trials for the treatment of TNBC, especially when associated with

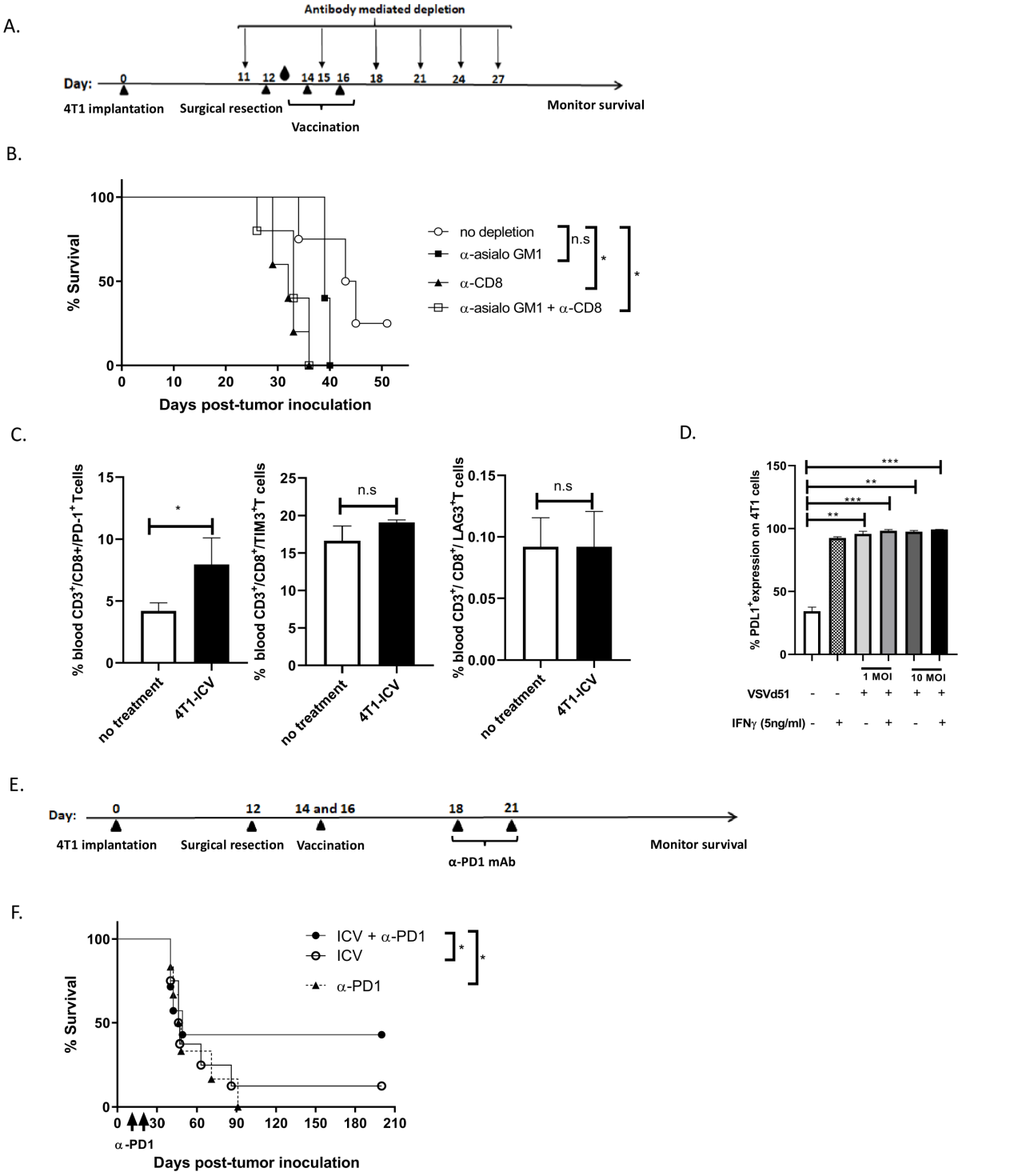

Figure 4 CD8$^+$ cytotoxic T cells are critical for infected cell vaccine (ICV) efficacy and combination treatment with anti-PD1 checkpoint inhibitor improves survival in BALB/c-4T1 model. (A) Timeline of immune cell depletion in the BALB/c-4T1 in vivo model. One day before surgical resection, NK cells, CD8$^+$ T cells and NK+CD8$^+$ T cells were depleted using antibodies to GM1, CD8 and GM1+CD8, respectively, and continued every 3–4 days for a total of 6 doses. On days 14 and 16, mice received 2 doses of ICV. Blood droplet denotes verification of in vivo depletion by flow cytometry. (B) Kaplan-Meier survival analysis of BALB/c mice bearing intramammary 4T1 tumors and receiving ICV and antibody depletion. n=10–12 mice/group. *p<0.05; n.s., not significant, log-rank test. (C) Single cell suspensions from the peripheral blood of mice following indicated treatments were stained with exhaustion markers on CD8$^+$ T cells (PD1, Tim3, LAG3) and analyzed by flow cytometry. All data are representative of three similar experiments where n=3–5 mice/treatment. *p<0.05; n.s., no significance. (D) Cell surface staining of PD-L1 on 4T1 cells following infection with VSVd51 in the presence or absence of IFNγ and analyzed by flow cytometry. (E) Timeline of combination therapy ICV+αPD1 in the BALB/c-4T1 in vivo model. Two days after vaccination, mice received 2 doses of anti-PD1 intraperitoneally 3 days apart. (F) Kaplan-Meier survival analysis of BALB/c mice bearing intramammary 4T1 tumors and receiving ICV and anti-PD-1. n=10–12 mice/group. *p<0.05; n.s., not significant, log-rank test.

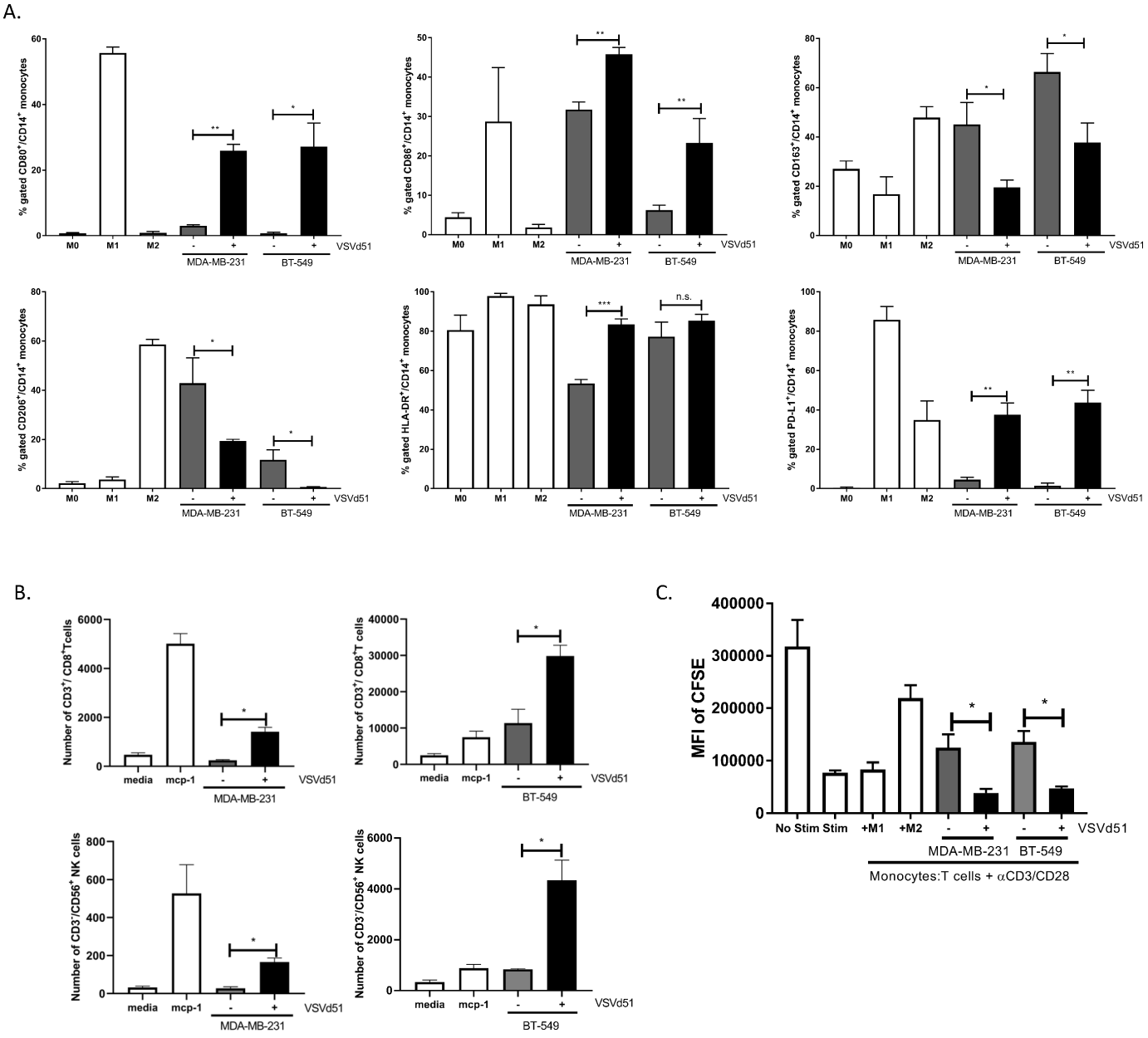

Figure 5 Polarization of human monocytes to M1 phenotype, increased migration of NK and CD8$^+$ T cells and increased proliferation of CD8$^+$ T cells following exposure to infected cell vaccine (ICV). (A) Polarization of purified human monocytes in the presence of conditioned media (CM) from human triple-negative breast cancer (TNBC) cell lines infected with VSVd51 (10 multiplicity of infection, 24 hours). Monocytes exposed to cytokines for control polarization as indicated. (B) Migration assay of purified human CD3$^+$/CD8$^+$ T cells and CD3$^-$/CD56$^+$ NK cells following exposure to CM of infected TNBC cells or controls as indicated. (C) CFSE-based proliferation assay of CD3$^+$/CD8$^+$ T cells following co-culture with human monocytes treated with CM or controls as indicated. All data are representative of at least three similar experiments where n=3 for technical replicates. *p<0.05; **p<0.01; ***p<0.001; n.s., not significant. MFI, mean fluorescence intensity.

homologous recombination deficiency.[43] Despite these new treatments, early data show modest improvements in survival, underscoring the need to improve therapeutic outcome for patients with TNBC.

Autologous tumor cell vaccines are an antigen agnostic form of personalized immunotherapy. Unlike single tumor antigen-targeted vaccines (pre-defined antigens), treatment with autologous tumor cell vaccines exposes a patient with cancer to their complete and individualized TAA repertoire, therefore reducing the likelihood of tumor escape due to tumor heterogeneity and eliminating the need to sequence the tumor a priori, saving both time and money.[18–20] The combination of cytokine delivery with whole tumor cells is capable of significantly delaying tumor growth through the creation of a pro-inflammatory environment to enhance immune system activation against TAAs.[44] Existing data suggest that disease recurrence is significantly delayed when patients successfully mount an immune response against the tumor, as evidenced by a delayed-type hypersensitivity response.[45]

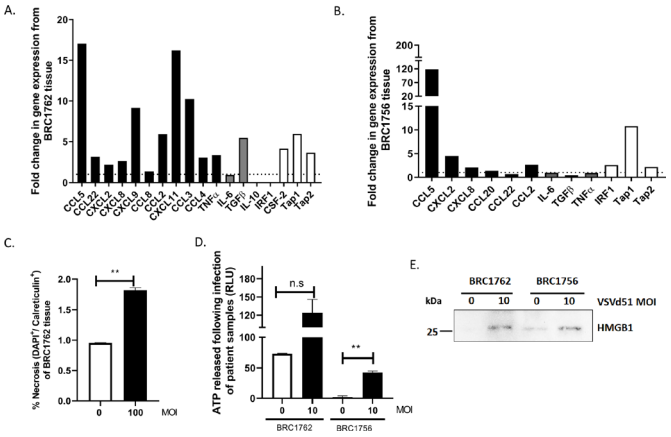

Figure 6 Infected cell vaccine (ICV) enhances immune signature and biomarkers of immunogenic cell death in human triple-negative breast cancer (TNBC) patient tissue. Fold change in gene expression from human TNBC patient tissue (A) BRC1762 and (B) BRC1756 following infection with VSVd51 at 10 multiplicity of infection (MOI) for 24 hours. (C) Measurements of cell surface calreticulin, (D) luminometry measurement of relative ATP and (E) Western blot analysis of HMGB1 from cell-free supernatants from TNBC patient tissue following infection with VSVd51 after 24 hours and at indicated MOI. Data are pooled from technical replicates, n=3, *p<0.05; **p<0.01; n.s., not significant.

Clinical studies have consistently shown that survival is significantly better in patients who mount an immune response against their tumor cells.[21 22] The strong immunological rationale for cytokine-based whole cell vaccines continues to drive the clinical development of this novel approach.[23–26] Unfortunately, the majority of patients do not mount such a response, either because the tumor cell vaccine and cytokine combination are not immunogenic enough or because the host immune system is suppressed in response to the cancer. The FANG vaccine, which is composed of granulocyte macrophage colony-stimulating factor/shRNAi furin vector-transfected autologous tumor cells, was designed to improve immunogenicity and dampen immune suppression.[46] Treatment with this vaccine was associated with a high rate of T-cell activation and prolonged recurrence-free survival in patients with stage III/IV ovarian cancer,[47] demonstrating the clinical potential of immunogenic autologous tumor vaccines.

Our laboratory and others have endeavored to improve on the whole cell vaccination paradigm by infecting tumor cells ex vivo with OV.[19–22] As proof of concept for solid tumors, we recently demonstrated that the intratumoral delivery of autologous colon cancer cells infected with rhabdoviral MG1 provided a significant therapeutic benefit to normally resistant mouse models of established peritoneal disease.[19] Both NK and T cells demonstrated enhanced recruitment to the peritoneal cavity following MG1-ICV administration.[19] From in vitro experiments in this study, we determined that infection of mouse and human TNBC cells with rhabdoviral VSVd51 results in higher necrotic cell death than in non-infected cells. We observed morphological features of necrosis by transmission EM, enhanced release of intracellular HMGB1 and ATP and increased calreticulin$^+$/DAPI$^+$ populations (figure 1). Further, an immunogenic gene signature was detected in infected TNBC cell lines. From in vivo experiments, we observed that postoperative vaccination of mice with 2 doses of ICV significantly augmented both innate and adaptive immune cell functionality. Both NK and CD8$^+$ T cells were important in contributing toward vaccine efficacy. However, CD8$^+$ T cells appear to play a more important role in mediating therapeutic efficacy as evidenced by shortened survival in CD8$^+$ T-cell-depleted mice, singly or in combination with NK cells.

In many cancer types, checkpoint blockade immunotherapy has been shown to provide long-lasting survival benefit by re-invigorating immune cells within the tumor; however, this occurs in only a small percentage of responding patients.[48–50] Resistance to checkpoint blockade therapy due to tumors evolving to escape immune attack further detracts from the clinical utility of this ground-breaking immunotherapy. As immunotherapy continues to reinforce itself at the forefront of oncology treatment, we strive to take advantage of these promising therapies by extending their clinical utility to immunogenically cold tumors such as TNBC. We propose to increase the recruitment of TILs into the TNBC tumor microenvironment through the use of immune-stimulatory combination immunotherapies. This could potentially be achieved through ICD-inducing chemotherapies such as doxorubicin or anthracyclines. Our in vitro and in vivo data showed that ICV is superior to drug treatment for enhancing ICD, immune recruitment and survival. However, this does not preclude the possibility of drug treatment with ICV prior to checkpoint blockade. Using ICD-inducing drug plus VSVd51-based ICV to initiate an anti-tumorigenic inflammatory response in TNBC tumors prior to treatment with checkpoint blockade has the potential to significantly improve patient prognosis by optimizing the power of complementary immunotherapy strategies. We envisage a future clinical trial to consist of an optimized adjuvant ICV-based strategy to initiate ICD and TAA release to promote an anti-tumor immune response. This will be followed by checkpoint inhibitor administration to further potentiate the anti-tumor activity of T cells at the tumor site. Our in vivo studies in BALB/c-4T1 mice showed improved and prolonged overall survival compared with monotherapy ICV or anti-PD1 alone. Immune profiling of other exhaustion markers on both NK and CD8$^+$ T cells following ICV treatment indicates that other checkpoint blockades including LAG3 on NK cells (data not shown) could be added to further improve the efficacy of this dual therapy. In a recent preclinical study to mimic the treatment course for patients with newly diagnosed TNBC, neoadjuvant OV was used to sensitize the tumor to checkpoint blockade therapy.[51] A neoadjuvant priming OV could potentially be administered prior to adjvuant ICV in a heterologous

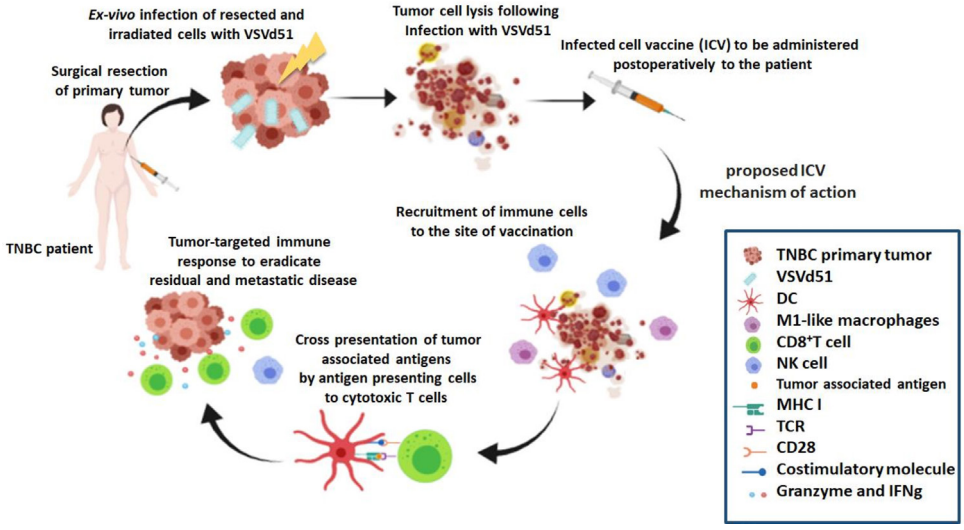

Figure 7 Proposed immune mechanism of action for ICV. Adjuvant vaccination with ICV results in the release of immunogenic cell death markers that recruit and activate innate and adaptive immune cells. Notably, antigen-presenting cells such as monocytes and dendritic cells (DCs) are primed to cross-present tumor-associated antigen to cytotoxic $CD8^+$ T cells. These adaptive immune T cells along with activated natural killer (NK) cells unleash tumor-targeted cytokines and cell death–inducing granules to reduce residual and metastatic triple-negative breast cancer (TNBC).

prime-boost strategy to achieve synergistic long-term anti-tumor benefits.

In human studies, we demonstrated that an analogous mechanism of ICV-induced immune activation is occurring in human TNBC cell lines and in human TNBC patient tumor samples. Our human TNBC cell line data demonstrate that ICV lysate can polarize monocytes toward an M1-like phenotype, induce maturation of DC (online supplementary figure 3A) and lead to greater NK and T-cell migration and T-cell proliferation (figure 5). In addition, qPCR data demonstrated upregulation of many genes that are involved in the immune process and the release of immunogenic DAMPs following infection of TNBC cell lines with VSVd51 (figure 2). In two TNBC patient samples, gene expression data revealed an immunogenic gene signature, while evaluation of ICD biomarkers showed augmented release of DAMPs following infection of patient tissue with VSVd51. Taken together, these human results demonstrate the feasibility of developing a VSVd51-based immunogenic vaccine to treat TNBC.

CONCLUSIONS

In summary, we characterized the mechanism and clinical potential of a VSVd51-based cancer vaccine for treating TNBC. We demonstrated that both innate and adaptive immune cells play mediating roles in the in vivo efficacy of ICV (figure 7). Further translational testing in our laboratory will include identifying ICD pathways intrinsic to individual TNBC patient tissue and their response to VSVd51 infection. This will allow us to engineer precision ICV to ensure that ICD is present, regardless of tumor heterogeneity, which is especially prevalent in the TNBC population. In addition, we aim to further understand the molecular events unleashed by ICV in our validated mice models and in patient samples that dictate immunogenicity and subsequent development of anti-tumor immunity. These translational studies could lead to future clinical trials of ICV monotherapy in TNBC or as potent anti-tumor immune response drivers in combination with immune checkpoint blockade. Although these studies are being conducted in TNBC, they have potential widespread implications across various solid tumor types.

Author affiliations
[1]Immunology and Cell Biology, Université de Sherbrooke, Faculté de médecine et des sciences de la santé, Sherbrooke, Quebec, Canada
[2]Pediatrics, Université de Sherbrooke, Faculté de médecine et des sciences de la santé, Sherbrooke, Quebec, Canada
[3]Pharmacology and Physiology, Université de Sherbrooke, Faculté de médecine et des sciences de la santé, Sherbrooke, Quebec, Canada
[4]Centre de recherche du CHUS, Sherbrooke, Quebec, Canada

Twitter Lee-Hwa Tai @TaiLabUdeS

Acknowledgements The authors would like to thank Francis Bernier-Godon, Isabelle Matte and Sylvie Turcotte for their assistance in processing blood and tumor tissue; Dr Denis Gris for immunofluorescence reagents; and Dr Leonid Volkov for their flow cytometry expertise.

Contributors S-RN, CL, MB, CS and L-HT executed experiments, read and approved the manuscript; S-RN and CL contributed in writing and critically revised the manuscript; L-HT conceived, designed and executed experiments, was a major contributor in writing the manuscript, and supervised the study. All authors have read and approved the manuscript.

Funding CIHR New Investigator Award and FRQS Jr 1 Salary Awards (L-HT)—provided salary for the principal investigator; CIHR Project Scheme Grant (L-HT)—provided operating funds for this study; Universite de Sherbrooke, Faculty of Medicine and Health Sciences Graduate Scholarship (S-RN)—provided the student scholarship for the first author.

Competing interests None declared.

Patient consent for publication Not required.

Ethics approval Mice were housed in pathogen-free conditions at the Central Animal Care Facility of the Université de Sherbrooke (Quebec). All studies and manipulations performed on animals were conducted in accordance with university guidelines and approved by the Faculty of Medicine Animal Care Committee at the university. Human tumor tissue was collected through the Sherbrooke Gynecological Biobank (VACS study, no. 2018-2414) and approved by the ethics board of CIUSSS de l'Estrie CHUS.

Provenance and peer review Not commissioned; externally peer reviewed.

Data availability statement The datasets used and/or analyzed during the current study are available from the corresponding author on reasonable request.

ORCID iD

Lee-Hwa Tai http://orcid.org/0000-0002-1176-4941

REFERENCES

1 Marra A, Viale G, Curigliano G. Recent advances in triple negative breast cancer: the immunotherapy era. *BMC Med* 2019;17:90.
2 Khosravi-Shahi P, Cabezón-Gutiérrez L, Custodio-Cabello S. Metastatic triple negative breast cancer: optimizing treatment options, new and emerging targeted therapies. *Asia Pac J Clin Oncol* 2018;14:32-39.
3 Lehmann BD, Pietenpol JA. Clinical implications of molecular heterogeneity in triple negative breast cancer. *Breast* 2015;24:S36–40.
4 Scully OJ, Bay B-H, Yip G, *et al*. Breast cancer metastasis. *Cancer Genomics Proteomics* 2012;9:311–20.
5 McAndrew N, DeMichele A. Neoadjuvant chemotherapy considerations in triple-negative breast cancer. *J Target Ther Cancer* 2018;7:52–69.
6 Karn T, Jiang T, Hatzis C, *et al*. Association between genomic metrics and immune infiltration in triple-negative breast cancer. *JAMA Oncol* 2017;3:1707.
7 Liu S, Lachapelle J, Leung S, *et al*. CD8+ lymphocyte infiltration is an independent favorable prognostic indicator in basal-like breast cancer. *Breast Cancer Res* 2012;14:R48.
8 Denkert C, Loibl S, Noske A, *et al*. Tumor-associated lymphocytes as an independent predictor of response to neoadjuvant chemotherapy in breast cancer. *J Clin Oncol* 2010;28:105–13.
9 Loi S, Michiels S, Salgado R, *et al*. Tumor infiltrating lymphocytes are prognostic in triple negative breast cancer and predictive for trastuzumab benefit in early breast cancer: results from the FinHER trial. *Ann Oncol* 2014;25:1544–50.
10 Budczies J, Bockmayr M, Denkert C, *et al*. Classical pathology and mutational load of breast cancer—integration of two worlds. *J Pathol Clin Res* 2015;1:225–38.
11 Banerji S, Cibulskis K, Rangel-Escareno C, *et al*. Sequence analysis of mutations and translocations across breast cancer subtypes. *Nature* 2012;486:405–9.
12 Lehmann BD, Jovanović B, Chen X, *et al*. Refinement of triple-negative breast cancer molecular subtypes: implications for neoadjuvant chemotherapy selection. *PLoS One* 2016;11:e0157368.
13 Lehmann BD, Bauer JA, Chen X, *et al*. Identification of human triple-negative breast cancer subtypes and preclinical models for selection of targeted therapies. *J Clin Invest* 2011;121:2750–67.
14 Lehmann BD, Pietenpol JA. Identification and use of biomarkers in treatment strategies for triple-negative breast cancer subtypes. *J Pathol* 2014;232:142–50.
15 Denkert C, Wienert S, Poterie A, *et al*. Standardized evaluation of tumor-infiltrating lymphocytes in breast cancer: results of the ring studies of the international immuno-oncology biomarker working group. *Mod Pathol* 2016;29:1155–64.
16 Salgado R, Denkert C, Demaria S, *et al*. The evaluation of tumor-infiltrating lymphocytes (TILs) in breast cancer: recommendations by an International TILs Working Group 2014. *Ann Oncol* 2015;26:259–71.
17 Keenan BP, Jaffee EM. Whole cell vaccines—past progress and future strategies. *Semin Oncol* 2012;39:276–86.
18 Cicchelero L, de Rooster H, Sanders NN. Various ways to improve whole cancer cell vaccines. *Expert Rev Vaccines* 2014;13:721–35.
19 Alkayyal AA, Tai L-H, Kennedy MA, *et al*. NK-cell recruitment is necessary for eradication of peritoneal carcinomatosis with an IL12-expressing Maraba virus cellular vaccine. *Cancer Immunol Res* 2017;5:211–21.
20 Prestwich RJ, Errington F, Steele LP, *et al*. Reciprocal human dendritic cell–natural killer cell interactions induce antitumor activity following tumor cell infection by oncolytic reovirus. *J Immunol* 2009;183:4312–21.
21 Guillerme J-B, Boisgerault N, Roulois D, *et al*. Measles virus vaccine-infected tumor cells induce tumor antigen cross-presentation by human plasmacytoid dendritic cells. *Clin Cancer Res* 2013;19:1147–58.
22 Lemay CG, Rintoul JL, Kus A, *et al*. Harnessing oncolytic virus-mediated antitumor immunity in an infected cell vaccine. *Mol Ther* 2012;20:1791–9.
23 Brun J, McManus D, Lefebvre C, *et al*. Identification of genetically modified Maraba virus as an oncolytic rhabdovirus. *Mol Ther* 2010;18:1440–9.
24 Stojdl DF, Lichty BD, tenOever BR, *et al*. VSV strains with defects in their ability to shutdown innate immunity are potent systemic anti-cancer agents. *Cancer Cell* 2003;4:263–75.
25 Bridle BW, Boudreau JE, Lichty BD, *et al*. Vesicular stomatitis virus as a novel cancer vaccine vector to prime antitumor immunity amenable to rapid boosting with adenovirus. *Mol Ther* 2009;17:1814–21.
26 Boudreau JE, Bridle BW, Stephenson KB, *et al*. Recombinant vesicular stomatitis virus transduction of dendritic cells enhances their ability to prime innate and adaptive antitumor immunity. *Mol Ther* 2009;17:1465–72.
27 Bridle BW, Stephenson KB, Boudreau JE, *et al*. Potentiating cancer immunotherapy using an oncolytic virus. *Mol Ther* 2010;18:1430–9.
28 Diaz RM, Galivo F, Kottke T, *et al*. Oncolytic immunovirotherapy for melanoma using vesicular stomatitis virus. *Cancer Res* 2007;67:2840–8.
29 Miest TS, Yaiw K-C, Frenzke M, *et al*. Envelope-chimeric entry-targeted measles virus escapes neutralization and achieves oncolysis. *Mol Ther* 2011;19:1813–20.
30 Patterson CE, Lawrence DMP, Echols LA, *et al*. Immune-mediated protection from measles virus-induced central nervous system disease is noncytolytic and gamma interferon dependent. *J Virol* 2002;76:4497–506.
31 Ockert D, Schirrmacher V, Beck N, *et al*. Newcastle disease virus-infected intact autologous tumor cell vaccine for adjuvant active specific immunotherapy of resected colorectal carcinoma. *Clin Cancer Res* 1996;2:21–8.
32 Schirrmacher V. Clinical trials of antitumor vaccination with an autologous tumor cell vaccine modified by virus infection: improvement of patient survival based on improved antitumor immune memory. *Cancer Immunol Immunother* 2005;54:587–98.
33 Conrad DP, Tsang J, Maclean M, *et al*. Leukemia cell-rhabdovirus vaccine: personalized immunotherapy for acute lymphoblastic leukemia. *Clin Cancer Res* 2013;19:3832–43.
34 Bertucci F, Gonçalves A. Immunotherapy in breast cancer: the emerging role of PD-1 and PD-L1. *Curr Oncol Rep* 2017;19:64.
35 Schmid P, Rugo HS, Adams S, *et al*. Atezolizumab plus nab-paclitaxel as first-line treatment for unresectable, locally advanced or metastatic triple-negative breast cancer (IMpassion130): updated efficacy results from a randomised, double-blind, placebo-controlled, phase 3 trial. *Lancet Oncol* 2020;21:44–59.
36 Tai L-H, de Souza CT, Bélanger S, *et al*. Preventing postoperative metastatic disease by inhibiting surgery-induced dysfunction in natural killer cells. *Cancer Res* 2013;73:97–107.
37 Tai L-H, Tanese de Souza C, Sahi S, *et al*. A mouse tumor model of surgical stress to explore the mechanisms of postoperative immunosuppression and evaluate novel perioperative immunotherapies. *J Vis Exp* 2014;85:1.
38 Garg AD, Galluzzi L, Apetoh L, *et al*. Molecular and translational classifications of DAMPs in immunogenic cell death. *Front Immunol* 2015;6:588.
39 Pitt JM, Kroemer G, Zitvogel L. Immunogenic and non-immunogenic cell death in the tumor microenvironment. *Adv Exp Med Biol* 2017;1036:65–79.
40 Erdag G, Schaefer JT, Smolkin ME, *et al*. Immunotype and immunohistologic characteristics of tumor-infiltrating immune cells are associated with clinical outcome in metastatic melanoma. *Cancer Res* 2012;72:1070–80.
41 Iannello A, Thompson TW, Ardolino M, *et al*. Immunosurveillance and immunotherapy of tumors by innate immune cells. *Curr Opin Immunol* 2016;38:52–8.
42 Nanda R, Chow LQM, Dees EC, *et al*. Pembrolizumab in patients with advanced triple-negative breast cancer: phase Ib KEYNOTE-012 study. *J Clin Oncol* 2016;34:2460–7.

43 Papadimitriou M, Mountzios G, Papadimitriou CA. The role of PARP inhibition in triple-negative breast cancer: unraveling the wide spectrum of synthetic lethality. *Cancer Treat Rev* 2018;67:34–44.
44 Slingluff CL, Petroni GR, Yamshchikov GV, *et al*. Clinical and immunologic results of a randomized phase II trial of vaccination using four melanoma peptides either administered in granulocyte-macrophage colony-stimulating factor in adjuvant or pulsed on dendritic cells. *J Clin Oncol* 2003;21:4016–26.
45 Disis ML, Schiffman K, Gooley TA, *et al*. Delayed-type hypersensitivity response is a predictor of peripheral blood T-cell immunity after HER-2/neu peptide immunization. *Clin Cancer Res* 2000;6:1347–50.
46 Senzer N, Barve M, Kuhn J, *et al*. Phase I trial of "bi-shRNAi(furin)/GMCSF DNA/autologous tumor cell" vaccine (FANG) in advanced cancer. *Mol Ther* 2012;20:679–86.
47 Nemunaitis J, Barve M, Orr D, *et al*. Summary of bi-shRNA/GM-CSF augmented autologous tumor cell immunotherapy (FANG™) in advanced cancer of the liver. *Oncology* 2014;87:21–9.
48 Trujillo JA, Sweis RF, Bao R, *et al*. T Cell-inflamed versus non-T cell-inflamed tumors: a conceptual framework for cancer immunotherapy drug development and combination therapy selection. *Cancer Immunol Res* 2018;6:990–1000.
49 Wei SC, Duffy CR, Allison JP. Fundamental mechanisms of immune checkpoint blockade therapy. *Cancer Discov* 2018;8:1069–86.
50 O'Donnell JS, Teng MWL, Smyth MJ. Cancer immunoediting and resistance to T cell-based immunotherapy. *Nat Rev Clin Oncol* 2019;16:151–67.
51 Bourgeois-Daigneault M-C, Roy DG, Aitken AS, *et al*. Neoadjuvant oncolytic virotherapy before surgery sensitizes triple-negative breast cancer to immune checkpoint therapy. *Sci Transl Med* 2018;10:1.